BIO-MIMETIC NANOSTRUCTURED SURFACES FOR NEAR-ZERO REFLECTION SUNRISE TO SUNSET

Stuart A. Boden* and Darren M. Bagnall[†]
Nanoscale Systems Integration
School of Electronics and Computer Science
University of Southampton, UK
*sb1@ecs.soton.ac.uk, +44 (0)23 8059 3737
[†]dmb@ecs.soton.ac.uk, +44 (0)23 8059 7609

Nanostructured moth-eye arrays for antireflective surfaces in silicon solar cells are investigated to confirm previously reported simulation results. A range of moth-eye arrays in silicon have been fabricated with periods from 150 nm to 350 nm. Reflectances of less than 0.5% were measured over a range of wavelengths from 550 nm to 870 nm. The moth-eye arrays are also compared with a thin-film antireflection coating and a micron-scale texturing scheme for a wide range of angles of incidence, to show that optically, these structures are excellent candidates for reducing reflection from solar cells.

Introduction

The high refractive index of silicon leads to the reflectance of between 30 and 50% of incident light across the useful part of the solar spectrum. In an effort to combat this, and so increase the power generated by a cell, thin films of dielectric material, in the form of single (SLAR) or double (DLAR) layer coatings (ARCs) are commonly used [1]. Destructive interference between light reflected from the interfaces created leads to lower reflectance but only for narrow ranges of wavelength and angle of incidence, dependent on the thickness and refractive index of the layers within the coating [2]. The wavelength range of useful solar radiation is large and throughout a day, direct sunlight is incident over a wide range of angles of incidence so thin-film coatings are not ideal methods of achieving antireflection for solar cells. There are also difficulties with the availability of materials with suitable optical properties and problems with delamination of layers. Thin films are often used in conjunction with micron-scale texturing in the form of pyramids, grooves or bowls to provide further reductions in reflectance [3, 4].

Texturing a silicon surface on the subwavelength scale is being investigated as an alternative to thin-film ARCs [5]. One approach has been to take inspiration from nature, where arrays of nanostructures are employed to confer an antireflective effect on the corneal surfaces and wings of certain species of moth [6-8]. Incident solar radiation cannot resolve the individual features of these so-called moth-eye arrays and so the patterns exhibit an effective refractive index dependent on the ratio of the corneal material to air. The features are shaped so that this ratio gradually increases from air into the cornea, leading to a gradual increase in effective refractive index. This eliminates the discontinuity in refractive index at the interface and so minimises reflection. Studies show that these surfaces exhibit low reflectivities over broad ranges of wavelength and angle of incidence ([9, 10]) and so could be more effective than thin film ARCs for reducing reflection over a day. We are investigating how the moth-eye principle can be exploited to provide antireflection for silicon solar cells. By analysing the effects of changing the geometry and arrangement of the features within the moth-eye array, we hope to develop an optimized structure that will reduce reflectance of solar radiation from sunrise to sunset.

Following promising simulation results (summary given here, for details see [11]) we fabricated moth-eye arrays in silicon using electron beam lithography and dry-etching. We then probed the reflectance properties of these structures.

Simulations

Simulations to assess the performance of thin film ARCs and moth-eye arrays for the ranges of wavelengths and angles of incidence experienced by real fixed solar cells over a full day have been carried out [11]. Reflectances were combined with solar spectra to determine the percentage of incident photons reflected from sunrise to sunset. These were also combined in PC1D to calculate the energy produced by a typical solar cell employing the

various AR schemes over a day.

Table I: Summary of results from simulations on silicon with various thin film and moth-eye antireflective surfaces [11].

Surface	Incident photons reflected over a day (%)	Extra Energy produced by 1 cm^2 cell over a day compared to one coated with a CeO SLAR (%)
SLAR (CeO)	18.2	-
DLAR (ZnS, MgF$_2$)	11.2	6.4
Moth-eye (250 nm)	11.7	5.3
Moth-eye (500 nm)	5.4	11.9

A summary of the results is given in Table I. The simulations show that moth-eye arrays with higher pillars exhibit lower reflectivities. A moth-eye array with a pillar height of 250 nm shows a similar performance to an optimized double layer ARC. Increasing the pillar height to 500 nm results in a reduction of the light reflected over a day to 5.4%. When compared to an optimized thin-film single layer ARC, a moth-eye array with a pillar height of 500 nm exhibits a 70% reduction in the light reflected from the surface, leading to a 12% increase in the energy produced by a solar cell over a full day.

Fabrication

The process used to fabricate moth-eye arrays in silicon is illustrated in Figure 1. Hexagonal arrays of spots were defined in ~100 nm thick Fox-12 (e-beam-sensitive flowable oxide from Dow Corning) on silicon. The period of the pattern was varied from 150 nm to 350 nm and the duty cycle (pillar width to period ratio) was varied from ~0.3 to ~0.7. Each pattern was limited to a 1 mm by 1 mm square to allow e-beam writing in a reasonable time. A HBr/Cl$_2$ anisotropic silicon dry etch was employed to transfer the pattern into the underlying silicon in the form of pillars with heights varying from ~150 nm to ~500 nm. A 20 nm thermal oxide was grown and then stripped off in an attempt to remove the damage caused by the dry etch- an important issue for minimizing surface recombination in solar cells- and to help form the desired moth-eye feature profile.
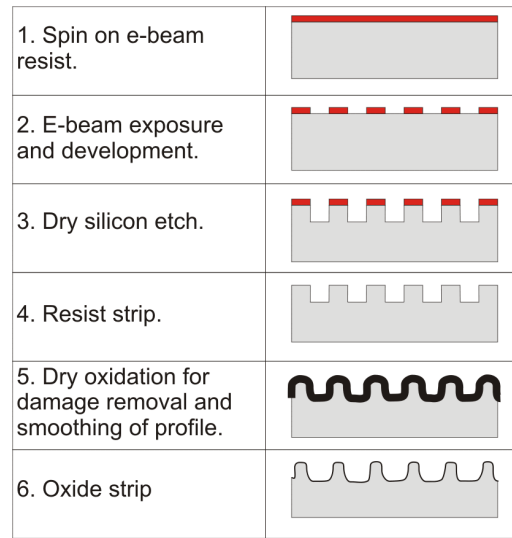

1. Spin on e-beam resist.	
2. E-beam exposure and development.	
3. Dry silicon etch.	
4. Resist strip.	
5. Dry oxidation for damage removal and smoothing of profile.	
6. Oxide strip	

Figure 1: Process for fabricating moth-eye arrays in silicon.

By carefully modulating the electron dose for each pattern, successful fabrication of moth-eye arrays in silicon was achieved. The micrograph in Figure 2 shows part of a moth-eye pattern (pillar period ~250 nm, duty cycle ~0.5, height ~350 nm) fabricated in silicon.

Optical Characterization

Reflectance from the fabricated moth-eye arrays was measured using a reflectance probe technique (see Figure 3). The probe (Ocean Optics) delivers light from a white light source (tungsten-halogen, Ocean Optics) to the sample through six optical fibres. A central optical fibre collects a proportion of light reflected from the sample and delivers this to a spectrometer (USB2000, Ocean Optics).
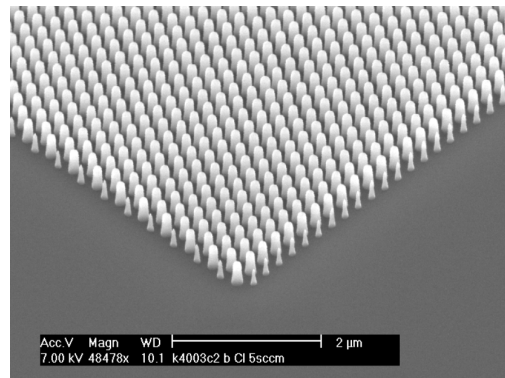

Figure 2: SEM micrograph of moth-eye array in silicon.

The distance between the probe tip and the sample was set to ensure that only light reflected from the 1 mm^2 patterned areas was collected by the spectrometer. Bare silicon was

used as a reflectance standard and the theoretical reflectance spectrum for this was used to produce graphs of absolute reflectance vs. wavelength.
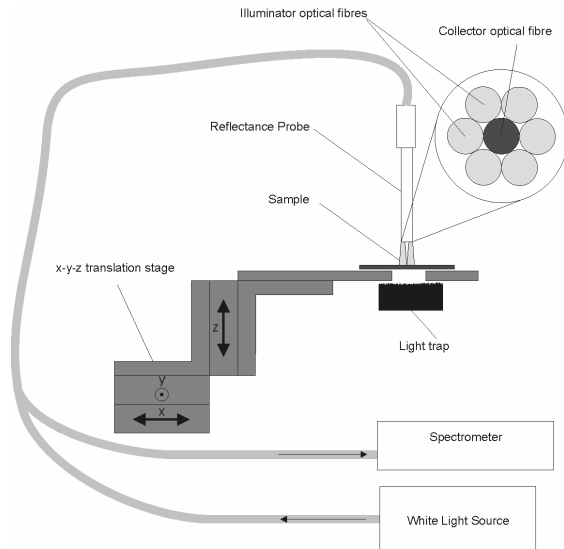

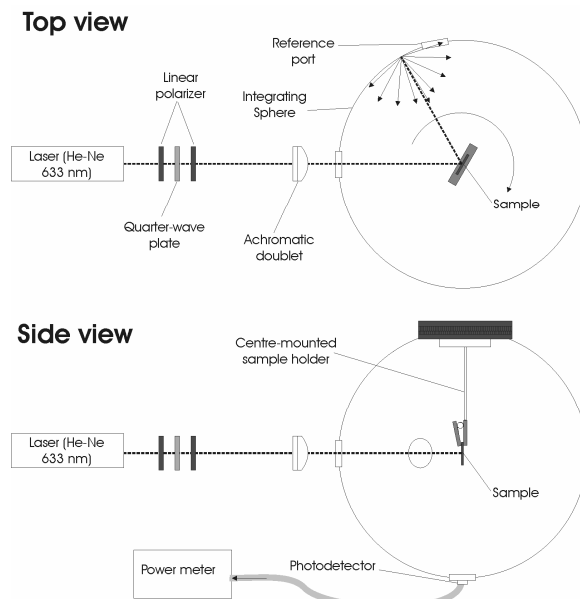**Figure 3:** Reflectance probe experiment.

Figure 4: Integrating sphere experiment for reflectance vs. angle of incidence measurements.

Reflectance vs. angle of incidence (AOI) measurements were performed using a 633 nm He-Ne Laser (Thorlabs) and an integrating sphere with a centrally-mounted sample holder (RTC-060-SF, Pro-lite (Labsphere)) (see Figure 4) Using a combination of linear polarizers and a quarter waveplate, the polarization of the incident laser light could be varied without substantially changing the intensity. Measurements were carried out for two orthogonal polarization states (s and p) and then the average was calculated as an indication of the behavior of the surfaces in randomly polarized light. An achromatic doublet lens was employed to focus the light to a small spot on the surface. The technique was used to compare a silicon moth-eye array with a bare silicon surface, and a silicon surface coated with a 100 nm thick SiO_2 SLAR. Measurements taken with an empty sample holder were used as a reference (R= 100%). Measurements were also taken using a secondary beam illuminating the sphere through the reflectance port to eliminated substitution errors.

Results and Discussion

Reflectance spectra from the probe experiments confirm the excellent antireflectivity of moth-eye arrays in silicon over a broad range of wavelengths (see Figure 5). Successfully fabricated moth-eye arrays with approximate pillar heights of 250, 400 and 500 nm exhibit reflectances that are substantially lower than that of a 100 nm SiO_2 SLAR (commonly used as an AR coating in silicon solar cells) across the whole range of wavelengths tested. For a pillar height of ~500 nm, the reflectance is below 0.5% from 550 nm to 870 nm. Increasing the pillar height leads to a decrease in the overall reflectance, as predicted by the simulations.

The integrating sphere measurements show that the moth-eye array exhibits excellent AR properties over a wide range of incident angles, with reflectances well below 5% for angles up to 50˚ (see Figure 6). It outperforms the other AR schemes for all tested angles. For comparison, results from a similar experiment performed by Parretta and colleagues [12] on a random micron-scale upright pyramids texture with an SLAR are included. The moth-eye array outperforms this texturing scheme for angles up to ~60˚. Beyond 60˚ the moth-eye reflectance curve rises sharply, above that of the micron-scale texturing scheme. However, the combination of the 1/cos(AOI) beam spread and the small area of the moth-eye samples (1 mm^2) may, at high angles, lead to the light being incident on some of the surrounding, unpatterned silicon, giving an anomalously high reflectance measurement. This is supported by the simulation results for the moth-eye array, also plotted in Figure 6, which predict, at high angles of incidence, lower reflectances than those measured. Further experiments with a reduced spot size or larger sample areas are required to investigate this.
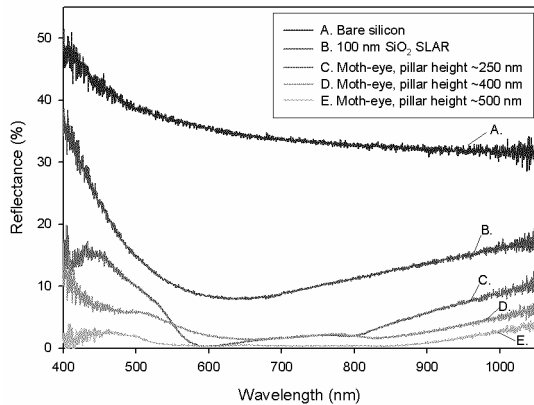
Figure 5: Reflectance probe experiments with various silicon surfaces. The period of the moth-eye arrays is 250 nm.
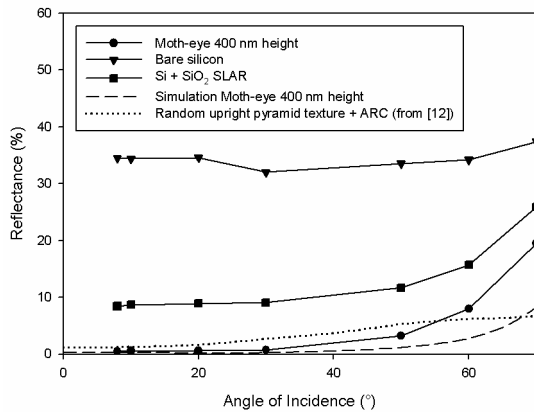

Figure 6: Reflectance versus angle of incidence results for silicon surfaces with various antireflective schemes.

For research purposes, larger areas could potentially be patterned in less time using more sensitive e-beam resists but e-beam lithography is not a commercially viable method for large scale implementation of moth-eye arrays in solar cells. However, with the rapid development of nanoimprinting and deep UV lithography technologies, we can now envisage cheap and reliable fabrication of such structures on solar cells.

Conclusion

Our simulations show that replacing a thin-film single layer ARC with a moth-eye array can result in a reduction of up to 70% in the light reflected from the surface, leading to a 12% increase in the amount of energy produced by a solar cell over a full day. We have successfully fabricated moth-eye structures in silicon and measurements using a reflectance probe technique confirm that these arrays have very low reflectances (<0.5%) over a broad range of wavelengths. Our integrating

sphere measurements of the variation of reflectance with angle of incidence show that a moth-eye array outperforms a micron-scale texturing scheme for AOIs up to 60° and we hope to show an improvement at even higher AOI with a more tightly focused beam or larger sample area. Our study suggests that moth-eye arrays are promising alternatives to thin film ARCs and micron-scale texturing for solar cell applications, giving very low reflectances over wide ranges of wavelength and incident angle. We believe that further improvements are possible by optimizing the pillar profile and arrangement.

References

[1] J. Zhao and M. A. Green, "Optimized Antireflection Coatings for High-Efficiency Silicon Solar-Cells," *IEEE Transactions on Electron Devices*, vol. 38, pp. 1925-1934, 1991.

[2] E. Hecht, *Optics*, 4th ed. San Francisco: Addison Wesley, 2002.

[3] P. Papet, O. Nichiporuk, A. Kaminski, Y. Rozier, J. Kraiem, J. F. Lelievre, A. Chaumartin, A. Fave, and M. Lemiti, "Pyramidal texturing of silicon solar cell with TMAH chemical anisotropic etching," *Solar Energy Materials and Solar Cells*, vol. 90, pp. 2319-28, 2006.

[4] J. Zhao, A. Wang, M. A. Green, and F. Ferrazza, "19.8% efficient 'honeycomb' textured multicrystalline and 24.4% monocrystalline silicon solar cells," *Applied Physics Letters*, vol. 73, pp. 1991, 1998.

[5] Y. Kanamori, M. Sasaki, and K. Hane, "Broadband antireflection gratings fabricated upon silicon substrates," *Optics Letters*, vol. 24, pp. 1422-1424, 1999.

[6] C. G. Bernhard, "Structural and functional adaption in a visual system," *Endeavour*, vol. 26, pp. 79-84, 1967.

[7] P. Vukusic and J. R. Sambles, "Photonic structures in biology," *Nature*, vol. 424, pp. 852-855, 2003.

[8] A. R. Parker, "515 million years of structural colour," *Journal of Optics a-Pure and Applied Optics*, vol. 2, pp. R15-R28, 2000.

[9] P. B. Clapham and M. C. Hutley, "Reduction of Lens Reflexion by the "Moth Eye" Principle," *Nature*, vol. 244, pp. 281-282, 1973.

[10] S. J. Wilson and M. C. Hutley, "The Optical-Properties of Moth Eye Antireflection Surfaces," *Optica Acta*, vol. 29, pp. 993-1009, 1982.

[11] S. A. Boden and D. M. Bagnall, "Biomimetic subwavelength surfaces for near-zero reflection sunrise to sunset," presented at 4th World Conference on Photovoltaic Energy Conversion, Hawaii, 2006.

[12] A. Parretta, A. Sarno, P. Tortora, H. Yakubu, P. Maddalena, Z. Jianhua, and W. Aihua, "Angle-dependent reflectance measurements on photovoltaic materials and solar cells," *Optics Communications*, vol. 172, pp. 139-51, 1999.